Journal of Power Sources 196 (2011) 3290–3295

Contents lists available at ScienceDirect

Journal of Power Sources

journal homepage: www.elsevier.com/locate/jpowsour

Preparation and characterization of core–shell battery materials for Li-ion batteries manufactured by substrate induced coagulation

Angelika Basch[a,*], Jörg H. Albering[b]

[a] Institute for Chemical Technology of Inorganic Materials, Graz University of Technology, A-8010 Graz, Austria
[b] Institute for Chemical Technology of Materials, Graz University of Technology, A-8010 Graz, Austria

ARTICLE INFO

Article history:
Received 25 August 2010
Received in revised form 13 October 2010
Accepted 7 November 2010
Available online 18 November 2010

Keywords:
Dip-coating
Core–shell
Lithium cobalt oxide
Li-ion battery
Titania

ABSTRACT

In this work Substrate Induced Coagulation (SIC) was used to coat the cathode material $LiCoO_2$, commonly used in Li-ion batteries, with fine nano-sized particulate titania. Substrate Induced Coagulation is a self-assembled dip-coating process capable of coating different surfaces with fine particulate materials from liquid media. A SIC coating consists of thin and rinse-prove layers of solid particles. An advantage of this dip-coating method is that the method is easy and cheap and that the materials can be handled by standard lab equipment. Here, the SIC coating of titania on $LiCoO_2$ is followed by a solid-state reaction forming new inorganic layers and a core–shell material, while keeping the content of active battery material high. This titania based coating was designed to confine the reaction of extensively delithiated (charged) $LiCoO_2$ and the electrolyte. The core–shell materials were characterized by SEM, XPS, XRD and Rietveld analysis.

1. Introduction

Currently, $LiCoO_2$ is the preferred cathode material for Li-ion batteries because it is easy to prepare, offers a good cycling stability and a good rate capability. Extensively delithiated (charged) $Li_{1-x}CoO_2$ (when $x \geq 0.5$) is prone to oxygen loss in the presence of an organic solvent, particulary when cells reach an operating temperature of 50 °C or more [1,2]. The high oxidizing power of delithiated $LiCoO_2$ causes oxidative decomposition of the electrolyte with the formation of polymeric films on the electrode surface [3]. It has been suggested in the past that surface coatings of $LiCoO_2$ with different oxides improve the cycling stability as well as the safety of overcharged and overheated Li-ion batteries, surpress phase transitions in the crystal structure and lead to a decrease in the disorder of cations in the cystal sites [4–7].

Cho et al. found that a better cycling stability for $LiCoO_2$ corresponding to a smaller lattice expansion along the *c*-axis, when coated with differernt metal-oxides [8]. The authors believe that oxides such as ZrO_2, Al_2O_3, TiO_2 or B_2O_3 react with $LiCoO_2$ and form a layer of $LiCo_{1-x}Al$ (or Zr, Ti, B)$_xO_2$ that is thought to suppress the expansion (and phase transition from hexagonal to monoclinic) during charging. Zhang et al. also reported that core–shell structured electrode materials can improve cycling behaviour [9]. Another group used Li_2SiO_3-coated $LiCoO_2$ in all solid-state cells to decrease the interfacial resistance on the electrode/electrolyte interface [10]. Other researchers have tried to improve Li_2SiO_3 rate capacity and cycling stability by coating the material with metal oxides such as MgO [11,12], SnO_2 [13], vanadium oxides (V_2O_5/V_2O_5 hydrates) [14], yttria-stabilized zirconia [15], Sb_2O_3-modified $Li_{1.1}CoO_2$ [16], a mixture of SrO/Li_2O/La_2O_3/Ta_2O_3/Ta_2O_5/TiO_2 [17], ZrO_2 [18,19], La_2O_3 [20], CeO_2 [21], Al_2O_3 [22–25], and $AlPO_4$ [26,27]. Another group studied the effect of Al doping on the cycling performance of $LiCoO_2$ [28].

The use of titania coatings using an in situ dipping and hydrolysing method to modify $LiCoO_2$-based electrodes with an improved cycling performance of $LiCo_{1/3}Ni_{1/3}MN_{1/3}O_2$ is described in [29,30,31]. Another group investigated the effects of La_2O_3/LiO_2/TiO_2 coatings on the electrochemical performance of $LiCoO_2$ cathodes [32] and MgO/TiO_2/SiO_2 [33].

The Substrate Induced Coagulation (SIC) coating process provides a self assembled and almost binder free coating with small particles. Most research so far has been used to coat a variety of surfaces with highly conductive carbon blacks [34,35,36]. Layers deposited by this technique have been used in electromagnetic wave shielding, in the metallization process of through-holes in printed wiring boards, and in the manufacture of conducting polymers (such as Teflon) [37,38,39]. An advantage of this dip-coating process is that it can be used for any kind of surface, provided the substrate is stable in water and that the particles used for the coating form a meta-stable dispersion. Recently, a non-aqueous SIC

* Corresponding author. Current address: Centre for Sustainable Energy Systems, The Australian National University, Building 32, North Road, Canberra ACT 0200, Australia. Tel.: +43 664 1773316.
E-mail address: angelika@basch.at (A. Basch).

0378-7753 © 2010 Elsevier B.V. Open access under CC BY-NC-ND license.
doi:10.1016/j.jpowsour.2010.11.043

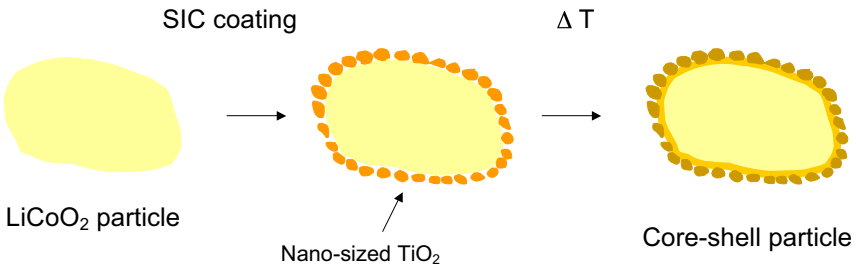

Fig. 1. Core–shell battery material forming $Li_x(M^a, M^b)O_2$ phases after SIC coating.

coating process of carbon black was developed by investigating the stabilities of non-aqueous dispersions [36]. These dispersions were used to prepare $LiCoO_2$-composite electrodes for Li-ion batteries with an improved conductivity while keeping the content of active battery material high [35].

Core–shell active materials based on $LiCoO_2$ have been prepared recently by the SIC of metal oxides to control oxdative processes at the cathode side [40]. This invention proposes that doping or partial substitution of Co in $LiCoO_2$ with other elements such as Al, Mg or Ti results in a structural stabilization especially for exensively delithiated (overcharged) material. Additionaly, the inventors found an improved cycling performance for Al_2O_3-coated $LiCoO_2$. Recently, the wetting characteristics and colloidal behaviour of nano-sized and dispersed titania have been investigated to find suitable conditions for an SIC process for titania [41] and alumina [52].

In this work we present the preparation of core–shell cathode-materials based on nano-sized TiO_2-coated $LiCoO_2$ by SIC (see Fig. 1) followed by a solid-state reaction. We analyse the materials thoroughly using a surface analysis techniques such as SEM and XPS and the bulk method XRD including Rietveld analysis.

2. Experimental

2.1. Preparation of core–shell battery materials by substrate induced coagulation

The mechanism of the SIC process was described first by Bele et al. [39]. The first step in the SIC process is to condition the substrate surface with a thin layer of polyelectrolyte or polymer. The substrate is then dipped into a metastable dispersion, which is stablized with a surfactant. The stability of the dispersion is optimized by adding electrolyte. Coagulation is induced by destabilization of the dispersion through interaction of the dispersed particles with the polyelectrolyte or polymer on the substrate surface.

The materials for the SIC process in this work were chosen in respect of their possible behaviour in a Li-ion battery. Polyvinylalcohol (PVA) was used as a conditioner to pretreat the cathode materials surface. In previous work the surface was pretreated with gelatin [39,38]. This is not suitable for application in Li-ion batteries as the presence of a protein may affect the redox-reaction because residues might lead to undesired side products, and as presence of sodium should be avoided. The conditioner – a 0.2 wt% PVA/solution – was prepared by dissolving 200 mg PVA (Mowiol 80-98, Hoechst) in 100 ml water at 60 °C. The solution was used at room temperature. The substrate, $LiCoO_2$ (Selectipur SC 15, Merck, 1.72010.1000), was conditioned by stirring 25 g in 50 ml of the PVA solution for 5 min. The conditioned powder was separated by filtration and washed 3 times with water. The dispersions were stabilized by the addition of Aerosol OT (dioctyl sulfosuccinate or bis-2-ethylhexyl sodium sulfosuccinate, $C_{20}H_{32}O_7SNa$ or AOT). For the preparation of the titania dispersion 1 g of titania (titanium dioxide P25, diameter 21 nm, Degussa) was added to a 2.7 mmol l^{-1} AOT and 40 mmol l^{-1} LiCl (Merck) solution in an elongated beaker. The dispersion was stirred for 5 min, sonicated (ultrasound) for 15 min, and stirred with a homogenizer for 10 min at >15 000 rpm. The beaker was covered with aluminium foil to stop the froth overflowing the container. The PVA-conditioned $LiCoO_2$ was stirred in the titania dispersion for 5 min, and separated from loose titania by filtration using a glass frit, so that the loose titania went through the filter with the supernatant. The powder was washed 3 times with water, filtered, and dried for 24 h at 60 °C. Although multiple coatings are possible using SIC – it has been shown previously that a carbon layer on electrodes produced by SIC can be prepared with a definded thickness by multible SIC coating [42] – the cathode material was single coated to keep the active battery material content high. The powder was dried under vacuum overnight and calcined for 3 h at 750 °C to perform a solid-state reaction on the lithium cobalt oxides surface.

2.2. Methods

2.2.1. Scanning electron microscopy (SEM)

Micrographs of the core–shell cathode material were taken using a CAMSCAN CF44 FESEM (field emission SEM) (Camscan, Cambridgeshire, UK). The samples were first coated using a carbon arc sputter coater, then imaged at various kinetic energies ranging from 7 to 15 kV. The sample was tilted 30 °C to the electron beam in the chamber to reduce effects of sample charging.

2.2.2. X-ray diffraction (XRD)

X-ray diffraction was used to get information about the crystallinity of the materals. The data was used for Rietveld refinement to characterize the phases after the solid-state reaction. The X-ray diffraction patterns used for the Rietveld refinement [43] were recorded using a Bruker-AXS D5005 with a secondary graphite monochromator and a scintillation counter using copper K_α radiation. The patterns were measured in a range of 10–90° 2-θ using a step-width of 0.02° and a speed of 20 s $step^{-1}$. The Rietveld refinement of metal-oxide coated samples was done performed over the range of 20–90° while using the package TOPAS R from Bruker-AXS.

2.2.3. X-ray photoelectron spectroscopy (XPS)

X-ray photoelectron spectroscopy measures the binding energy of electrons in a solid. An electron's binding energy is characteristic of the atom from which it was emitted and can be obtained by observing the photo-electron spectrum. Furthermore, the photoelectron peaks exhibit second order effects, often referred to as chemical shifts, which reflect the oxidation state of the parent atom and the electronegativities of surrounding atoms. As the area under each peak is proportional to the concentration of the parent atom, XPS can also provide atomic concentrations of elements on the surface [44]. X-ray photoelectron spectra were recorded using a Physical Electronics PHI 5400 spectrometer, with a Mg K_α radiation source ($h\nu$ = 1253.6 eV) operating at 15 kV and 300 W. The X-ray source was not monochromated. Survey spectra were recorded for the region 0–1100 eV at a pass energy of 93.9 eV and resolution of

0.4 eV step^{-1}. Multiplex spectra were recorded for selected photoelectron peaks at a pass energy of 29.35 eV and resolution of 0.125 eV step^{-1}. During each analysis, the sample stage was cooled with liquid nitrogen to provide a base pressure of 5×10^{-8} Torr inside the sample chamber. Because of the insulating properties of some of the samples, these became charged during analysis, causing the photoelectron peaks to shift to artificially high binding energy. The amount of charge shift was determined from the observed binding energy of the C–H component to the C 1s peak, which has a value of 284.8 ± 0.2 eV before charging [45]. The charging can be compensated by a neutralizer, which floods the surface of the sample with low-energy electrons. All binding energies listed in this report have been corrected for charging. Atomic concentrations were obtained from the experimental peak area using the atomic sensitivity factor of each element [46].

3. Results and discussion

3.1. Morphology of titania coating on lithium cobalt oxide

The morphology of uncoated $LiCoO_2$ is shown in Fig. 2 and did not change after heating. However, after a SIC coating the titania layer seems to be quite dense and covers much of the $LiCoO_2$-particle surface, as seen in Figs. 3 and 4. The calcined core–shell material is shown in Fig. 5. At higher magnification, it can be seen that calcination leads to a change in the morphology of the coating

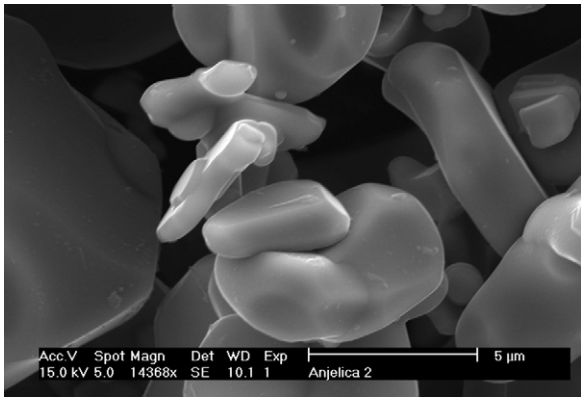

Fig. 2. Uncoated cathode material $LiCoO_2$. Scale bar is 5 μm.

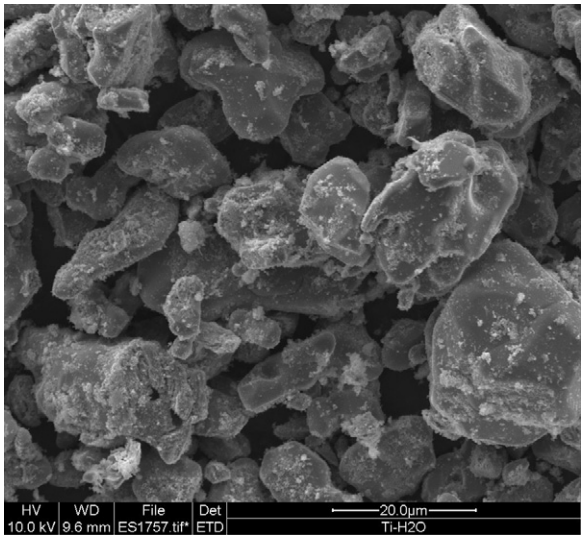

Fig. 3. SEM image of $LiCoO_2$ coated with TiO_2 by aqueous SIC. Scale bar is 20 μm.

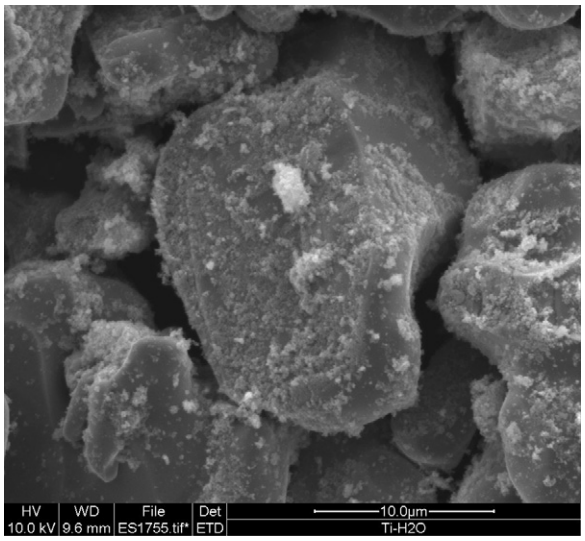

Fig. 4. SEM image of $LiCoO_2$ coated with TiO_2 aqueous SIC. Scale bar is 10 μm.

shown in Fig. 6. A magnification of the calcined titania layer displayed in Fig. 7 shows that the coating appears not to be completely dense.

3.2. Phases of core–shell battery material

Fig. 8 displays the X-ray difraction pattern (blue line) and the Rietveld analysis (red line) fitted to the XRD pattern of the core–shell material after the solid-state reaction. Due to the results optaind from Rietveld analysis a single SIC coating followed by a calcination step leads to three phases: 87.88% $LiCoO_2$, 5.19% spinel Co_3O_4 and 6.93% Li_2TiO_3. The content of $LiCoO_2$ in the bulk might be higher than the calculated value by Rietveld methods, since the depth of penetration of the X-rays might be lower than the grain size of a significant fraction of the sample, resulting in artificially increased ratio of the phases agglomerated at the grain surface. The hexagonal lattice constants given in Table 1 of the bulky $LiCoO_2$ remain unchanged after the calcination and are in good accordance with data reported in the literature (e.g. Takahashi et al., $a = 281.56(6)$ pm, $c = 1405.42(6)$ pm [47]). Thus, it can be concluded

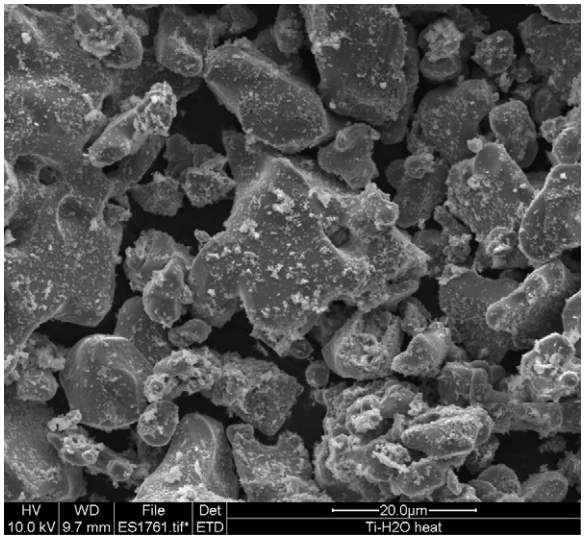

Fig. 5. SEM image of $LiCoO_2$ coated with TiO_2 aqueous SIC and then calcined. Scale bar is 20 μm.

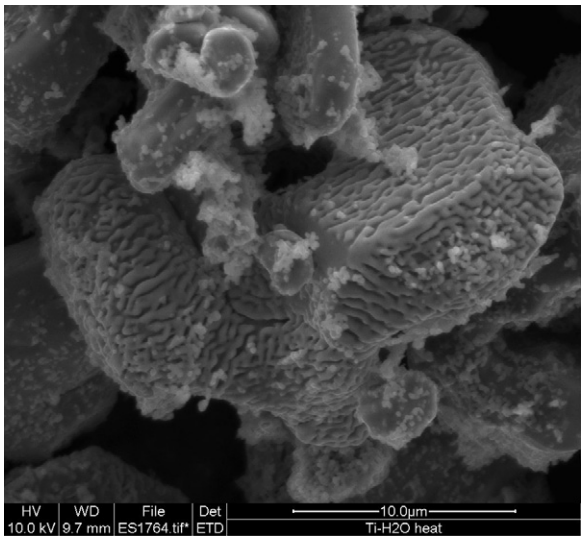

Fig. 6. SEM image of $LiCoO_2$ coated with TiO_2 aqueous SIC and then calcined. Scale bar is 10 μm.

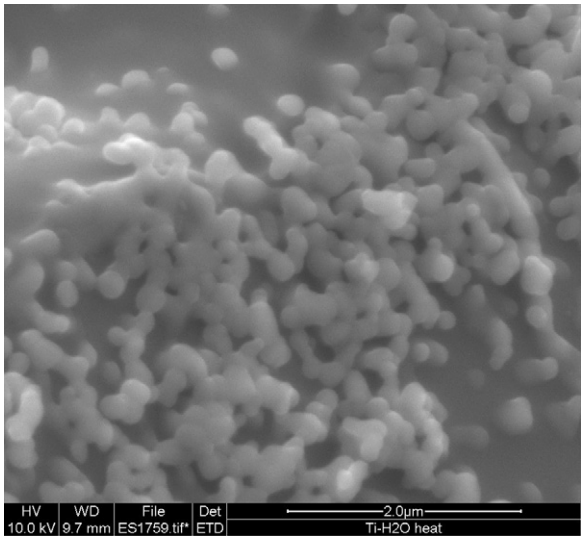

Fig. 7. SEM image of $LiCoO_2$ coated with TiO_2 aqueous SIC and then calcined. Scale bar is 2 μm.

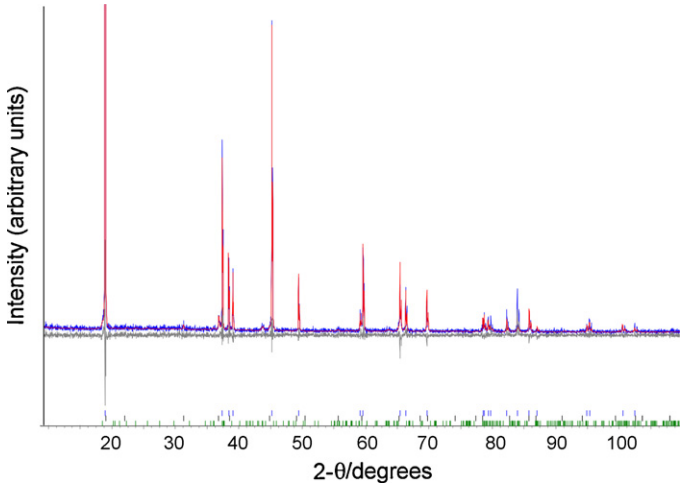

Fig. 8. X-ray diffraction pattern (blue line) and Rietveld analysis (red line) of calcined titania-coated $LiCoO_2$. The grey line shows the difference between the measured and the calculated pattern. (For interpretation of the references to color in this figure legend, the reader is referred to the web version of the article.)

Table 1
Phases of calcined titania-coated $LiCoO_2$.

Phase	Space group	Lattice parameter
$LiCoO_2$	$R\bar{3}m$ (166)	a = 281.62(1) pm c = 1404.95 pm
Co_3o_4	$F\bar{4}3m$ (216)	a = 807.0(1) pm
Li_2TiO_3	$C2/c$ (15)	a = 508.6(8) pm b = 878(1) pm c = 971(2) pm β = 99.9(1)°

that the reaction of the titania coating with $LiCoO_2$ does take place only at the surface of the grains, and should therefore have little effect on the electrochemical bulk capacity of the electroactive material. Li_2TiO_3 crystallizes with its own, easily identifiable, structure type. The lattice constants of this compound, also given in Table 1, are in good agreement with the data obtained from a single crystal structure determination (a = 504.1(2) pm, b = 880.6(2) pm, c = 972.7(2) pm β = 100.008(50)°, Dorrian and Newnham [48]). The third component, Co_3O_4, is a spinel type compound with a cubic lattice constant of a = 807.0(1) pm. This value is close to reported data for Co_3O_4 (e.g. a = 808.21(1) pm, Liu and Prewitt [49]) and does not correspond to a compound $TiCo_2O_4$ (a = 844.3(1) pm, Hirota et al. [50]). Kosova and Devyatkina also found a small amount of Co_3O_4, after coating $LiCoO_2$ with Al_2O_3 [4]. It may be plausible that a certain fraction of lithium remains in the crystal lattice of the spinel type compound, thus forming a compound $Li_xCo_{3-x}o_4$. However, the value of x probably is small, since the Rietveld refinement did not show unusually high displacement parameters for the metal sites of the spinel structure. This would be the case if lithium replaces cobalt in a large fraction of the structure. Given these findings, the reaction between titania and $LiCoO_2$ can be roughly expressed by the following equation:

$$12LiCoO_2 + 6TiO_2 \rightarrow 6Li_2TiO_3 + 4Co_3O_4 + O_2$$

The evolution of oxygen during the reaction is a consequence of the partial reduction of Co^{3+} to Co^{2+} during the formation of the spinel component. A layer of $LiCo_{1-x}Ti_xO_2$, as proposed by Cho et al. was not detected [8].

3.3. Surface composition of core–shell battery materials

The binding energies of electrons in elements in the titania coating for both the calcined and uncalcined samples, as well as titania and uncoated $LiCoO_2$, were measured by XPS.

The titania-coated sample showed a higher surface concentration of both O and Ti on the materials surface compared to titania-coated and calcined $LiCoO_2$, whereas the Co concentration was decreased as shown in Table 2. Calcining the sample leads to a further decrease of the Co surface concentration. Li has only a single core–shell, the 1s, and so only produces a single photoelectron peak, the intensity of which is very low because of its low sensitivity factor. In the spectra of the titania coated materials, the Li 1s peak was obscured by the satellite peak from the Co 3p/Ti 3s peak.

Table 2
Element surface concentrations (atom%) for pristine $LiCoO_2$, pristine TiO_2, coated $LiCoO_2$, and coated $LiCoO_2$ after heating optained by XPS.

Element	$LiCoO_2$	TiO_2	TiO_2 coated $LiCoO_2$	TiO_2 coated $LiCoO_2$, calcined
C	27.8	15.1	15.7	20.1
O	47.1	60.5	59.5	55.9
Ti	–	24.4	13.1	8.3
Co	12.9	–	11.7	9.0
Li	(12.2)	(–)	(–)	(6.8)

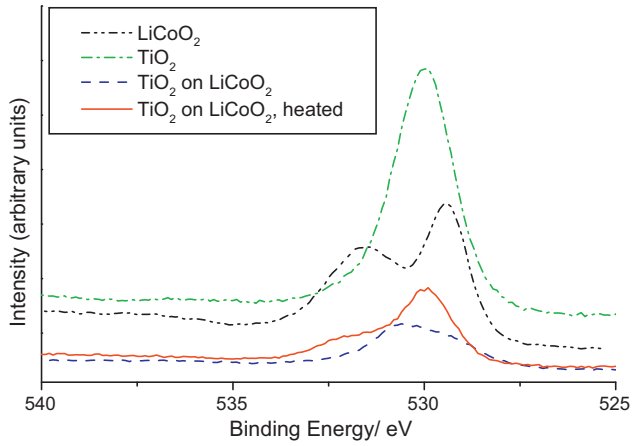

Fig. 9. X-ray photoelectron spectrum of the O 1s regions of $LiCoO_2$ (black, dashed and double-dotted), titania (green, dashed and dotted), titania coated $LiCoO_2$ (blue, dashed), and calcined titania-coated $LiCoO_2$ (red, solid). (For interpretation of the references to color in this figure legend, the reader is referred to the web version of the article.)

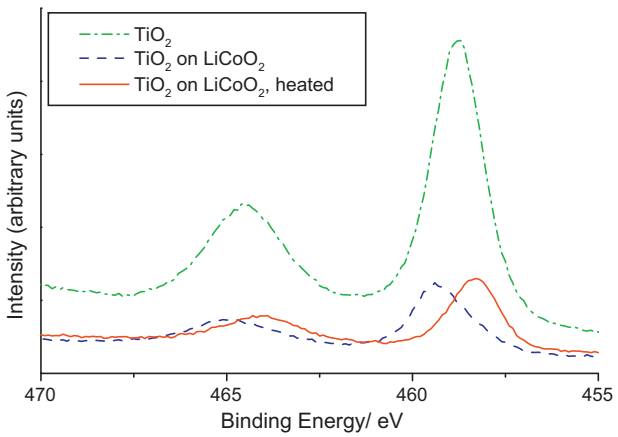

Fig. 11. X-ray photoelectron spectrum of the Ti 2p regions of titania (green, dashed and dotted), titania coated $LiCoO_2$ (blue, dashed), and calcined titania-coated $LiCoO_2$ (red, solid). (For interpretation of the references to color in this figure legend, the reader is referred to the web version of the article.)

The satellite arises because the X-ray source was not monochromated, so some low-intensity Mg $K\alpha_{3,4}$ radiation is emitted along with the principal Mg $K\alpha_{1,2}$ radiation. Because of this overlap, it was not possible to determine the area under the Li 1s peak and, consequently, the surface concentration of Li. As a result, it is not possible to determine the trend in the surface concentration of Li. Because of this overlap the surface concentration is not accurate and indicated by brackets in Table 2. Peaks of carbon (C) are found in all samples found because of adventitious hydrocarbon contamination.

A detailed analysis of the O 1s and Co 2p spectra of uncoated $LiCoO_2$ are given by by Daheron et al. [51].

Fig. 9 shows the X-ray photoelectron spectra of the O 1s region of the uncalcined (blue, dashed) and the calcined sample (red, solid), at least three components in resulting from both $LiCoO_2$ and TiO_2 were detected. The spectra of $LiCoO_2$, the unheated, and the heated sample show a doublet at 795.0 and 779.5 eV in the Co 2p region and an additional component at lower binding energy at 789.7 eV. Fig. 10 shows the Co 2p regions where the unheated sample (blue, dashed) as well as the heated (red, solid) shows just one for each peak in the doublet. In the Ti 2p region – displayed in Fig. 11 – a doublet was found for the unheated sample (blue, dashed) at 465.0 and 459.5 eV and at lower binding energies at 464.0 and 458.3 for the heated sample (red, solid). The photoelectron peaks in the spectra of the calcined sample were split if the spectrum was recorded with the neutralizer off. This splitting disappeared when the spectra were recorded with the neutralizer on. This can just happen if parts of the sample are charging and others are not. This implies that parts of the sample were more insulating than others. It is possible that this is because the particles are not evenly or completely coated. This effect was only observed for the calcined samples. No neutralizer was needed during measurements for $LiCoO_2$ and TiO_2.

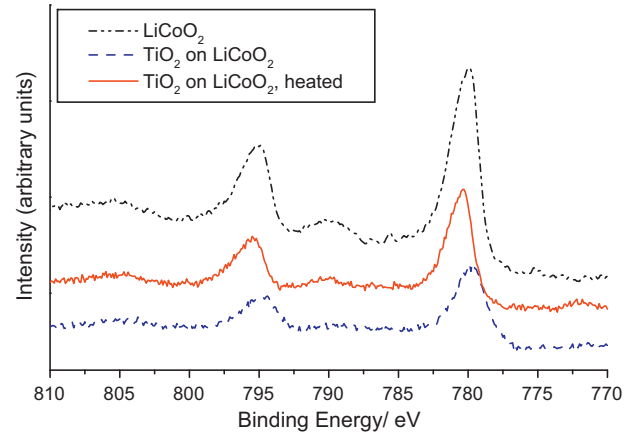

Fig. 10. X-ray photoelectron spectrum of the Co 2p regions of $LiCoO_2$ (black, and double-dotted), titania coated $LiCoO_2$ (blue, dashed), and calcined titania-coated $LiCoO_2$ (red, solid). (For interpretation of the references to color in this figure legend, the reader is referred to the web version of the article.)

4. Conclusion and outlook

Substrate Induced Coagulation (SIC) is a suitable method to prepare core–shell battery materials with a thin and dense layer of nano-sized particles as depicted by SEM. It was shown by XPS and XRD data that the materials form new crystalline phases on the surface after a solid state reaction was initiated. The reaction of titania with the battery material takes place only at the surface and should therefore have little effect on the electrochemical bulk capacity and the electroactive material. It was clearly shown by the Rietveld refinement of XRD powder patterns that after a single SIC coating the content of the active material is kept high. We therefore belive that the presented core–shell battery material might show an improved cycling performance. The electrochemical properties of this material will be adressed in future research.

Acknowledgements

This work was supported by the Austrian Science Fund (FWF) in the Special Research Program "Electroactive Materials" and project J 2979. The authors would like to thank Jürgen O. Besenhard (Graz University of Technology, Austria) for his guidance in the beginning of this project at the Institute for Chemical Technology of Inorganic Materials (Graz University of Technology, Austria) as well as Robert T. Jones (University of South Australia, Adelaide, Australia) for XPS measurements, Angus Netting (University of South Australia, Adelaide, Australia) and Julian Wagner (Centre for Electron Microscopy Graz, Graz University of Technology, Austria) for SEM measurements and Hermann-Josef Schimper (TU Darmstadt, Germany) and Fiona Beck (The Australian National University, Australia) for useful discussions.

References

[1] B. Scrosati, J. Garche, Journal of Power Sources 195 (2010) 2419.
[2] R. Alcantara, P. Lavela, J.L. Tirado, E. Zhecheva, R. Stoyanova, Journal of Materials Science Letters 3 (1999) 121.
[3] M. Winter, J.O. Besenhard, M.E. Spahr, P. Novák, Advanced Materials 10 (1998) 725.
[4] N.V. Kosova, E.T. Devyatkina, Journal of Power Sources 174 (2007) 959.
[5] C. Li, H.P. Zhang, L.J. Fu, H. Liu, Y.P. Wu, E. Ram, R. Holze, H.Q. Wu, Electrochimica Acta 51 (2006) 3872.
[6] L.J. Fu, H. Liu, C. Li, Y.P. Wu, E. Rahm, R. Holze, H.Q. Wu, Solid State Sciences 179 (2006) 113.
[7] T. Ohzuku, in: J.O. Besenhard (Ed.), Handbook of Battery Materials, Wiley-VCH, Weinheim, Germany, 1999.
[8] J. Cho, Y.-J. Kim, T.-J. Kim, B. Park, Angewandte Chemie International Edition 40 (18) (2001) 3367.
[9] H.P. Zhang, L.C. Yang, L.J. Fu, Q. Cao, D.L. Sun, Y.P. Wu, R. Holze, Journal of Solid State Electrochemistry 13 (2008) 1521.
[10] A. Sakuda, H. Kitaura, A. Hayashi, K. Tadanaga, M. Tatsumisago, Journal of the Electrochemical Society 156 (2009) A27.
[11] M. Mladenov, R. Stoyanova, E. Zhecheva, S. Vassilev, Electrochemistry Communications 3 (2001) 410.
[12] Z. Wang, X. Huang, L. Chen, Journal of the Electrochemical Society 150 (2) (2003) A199.
[13] J. Cho, C.-S. Kim, S.-I. Yoo, Electrochemical and Solid-State Letters 3 (8) (2000) 362.
[14] J.W. Lee, S.M. Park, H.J. Kim, Journal of Power Sources 188 (2009) 583.
[15] G.T.K. Fey, C.L. Hsiao, P. Muralidharan, Journal of Power Sources 189 (2009) 837.
[16] J.P. Yu, X.H. Hu, H. Zhan, Y.H. Zhou, Journal of Power Sources 189 (2009) 697.
[17] H. Wang, Z.Q. Deng, M.C. Chen, Journal of Rare Earths 27 (2009) 234.
[18] K.Y. Chung, W.S. Yoon, J. McBreen, X.Q. Yang, S.H. Oh, W.H. Ryu, J.L. Lee, I.C. Won, B.W. Cho, Journal of Power Sources 163 (2006) 185.
[19] K.Y. Chung, W.S. Yoon, J. McBreen, X.Q. Yang, S.H. Oh, H.C. Shin, W.I. Cho, B.W. Cho, Journal of the Electrochemical Society 153 (2006) A2152.
[20] G.T.K. Fey, P. Muralidharan, C.Z. Lu, Y.D. Cho, Electrochimica Acta 189 (2009) 837.
[21] H.W. Ha, N.J. Yun, M.H. Kim, M.H. Woo, K. Kim, Electrochimica Acta 51 (2006) 3297.
[22] N. Kosova, E. Devyatkina, A. Slobodyuk, V. Kaichev, Solid State Ionics 179 (2008) 1745.
[23] J. Cho, Y.J. Kim, B. Park, Chemistry of Materials 12 (2000) 3788.
[24] L. Liu, Z. Wang, H. Li, L. Chen, X. Huang, Solid State Ionics 152–153 (2002) 341.
[25] Z. Wang, L. Liu, H. Li, L. Chen, X. Huang, Solid State Ionics 148 (2002) 335.
[26] J. Cho, Electrochemistry Communications 5 (2003) 146.
[27] J. Cho, B. Kim, J.-G. Lee, Y.-W. Kim, B. Park, Journal of the Electrochemical Society 152 (1) (2005) A32.
[28] S.-T. Myung, N. Kumagai, S. Komaba, H.-T. Chung, Solid State Ionics 139 (2001) 47.
[29] F. Wu, M. Wang, Y.F. Su, S. Chen, Acta Physico-Chimica Sinica 25 (2009) 629.
[30] F. Wu, M. Wang, Y.F. Su, S. Chen, B. Xu, Solid State Ionics 179 (2006) 1745.
[31] Y.D. Chen, Y. Zhao, Q.Y. Lai, N.N. Wei, J.Z. Lu, X.G. Hu, X.Y. Ji, Ionics 14 (2008) 53.
[32] W. Hong, M.C. Chen, Journal of Rare Earths 25 (2007) 124.
[33] W. Hong, M.C. Chen, Electrochemical Solid State Letters 9 (2006) A82.
[34] M. Bele, Ph.D. thesis, Univerza Ljubljani, 1997.
[35] A. Basch, B. Gollas, R. Horn, J.O. Besenhard, Journal of Applied Electrochemistry 35 (2005) 169.
[36] A. Basch, R. Horn, J.O. Besenhard, Colloids and Surfaces A: Physicochemical and Engineering Aspects 253 (2005) 155.
[37] J.O. Besenhard, S. Hanna, C. Hagg, D. Fiedler, M. Bele, S. Pejovnik, H. Meyer, in: H. Rathore, G. Mathad, C. Plougonven, C. Schuckert (Eds.), Proc. Electrochem. Soc., Interconnect and Contact Metallization, vol. PV 97-31, 1997, pp. 96–107.
[38] M. Bele, K. Kocevar, S. Pejovnik, J.O. Besenhard, I. Musevic, Colloids and Surfaces 168 (2000) 231.
[39] M. Bele, K. Kocevar, S. Pejovnik, J.O. Besenhard, I. Musevic, Langmuir 16 (2000) 8334.
[40] J.O. Besenhard, M. Wachtler, J.-H. Han, A. Basch, US 2004/0258836, 2004.
[41] A. Basch, S. Strnad, V. Ribitsch, Colloids and Surfaces A: Physicochemical and Engineering Aspects 333 (2009) 163.
[42] K.W. Leitner, J.O. Besenhard, M. Winter, Journal of Power Sources 146 (1–2) (2005) 209.
[43] R.A. Young, The Rietveld Method, 1993, pp. 886–889.
[44] D.J. O'Connor, B.A. Sexton (Eds.), R.S.C.S. Surface Analysis Methods in Materials Science, 1992.
[45] D. Briggs, M.P. Seah, Practical Surface Analysis, vol. 1, Appendix 2, 1993.
[46] J.F. Moulder, W.F. Stickle, P.E. Sobol, K.D. Bomben, Physical Electronics, Inc, USA, 1995.
[47] Y. Takahashi, N. Kijima, K. Dokko, M. Nishizawa, I. Uchida, J. Akimoto, Solid State Chemistry 180 (1) (2007) 313.
[48] J.F. Dorrian, R.E. Newnham, Materials Research Bulletin 4 (1969) 179–184.
[49] X. Liu, C.T. Prewitt, Physics and Chemistry of Minerals 4 (1969) 179–184.
[50] K. Hirota, T. Inoue, N. Mochida, A. Ohtsuka, Powder Diffraction 4 (1989) 40–45.
[51] L. Daheron, H. Martinez, R. Deryvere, I. Baraille, M. Menetier, C. Denage, C. Delmas, D. Gonbeau, Journal of Physical Chemistry C 113 (2009) 5843.
[52] A. Basch, S. Strnad, Colloids and Surfaces A: Physicochemical and Engineering Aspects (2010) in press, doi:10.1016/j.colsurfa.2010.10.026.